CFD Letters 11, Issue 12 (2019) 21-33

CFD Letters

Journal homepage: www.akademiabaru.com/cfdl.html
ISSN: 2180-1363

Effect of Suction/Injection on Stagnation Point Flow of Hybrid Nanofluid over an Exponentially Shrinking Sheet with Stability Analysis

Open Access

Nur Syazana Anuar[1,*], Norfifah Bachok[1,2], Norihan Md Arifin[1,2], Haliza Rosali[1]

[1] Department of Mathematics, Faculty of Science, Universiti Putra Malaysia, 43400 UPM Serdang, Selangor, Malaysia
[2] Institute for Mathematical Research, Universiti Putra Malaysia, 43400, UPM Serdang, Selangor, Malaysia

ARTICLE INFO

Article history:
Received 20 October 2019
Received in revised form 15 December 2019
Accepted 20 December 2019
Available online 28 December 2019

Keywords:
Hybrid Nanofluid; Suction/Injection; Dual Solutions; Stability Analysis

ABSTRACT

This research aims to investigate the effect of suction/injection on the stagnation point flow over an exponentially shrinking sheet in a hybrid nanofluid. It is worth to mention that hybrid nanofluids are formed by adding the mixture of Ag nanoparticles into a CuO/water nanofluid. The governing boundary layer equations are transformed into an ordinary differential equation using a similarity variable. The features of the flow and heat transfer characteristic for various values of suction/injection parameter, nanoparticle volume fraction parameter and shrinking parameter are presented graphically and discussed. The results acquired are in good agreement with previously published results. Non-unique (more than one) solutions are visible for a certain range of shrinking parameter. Hence, a stability analysis is performed to identify the stability of solutions obtained. Therefore, it is confirmed that the first solution is stable whereas the second solution is unstable. It is revealed that the heat transfer rate of hybrid nanofluid is greater compared to regular nanofluid.

1. Introduction

Hybrid nanofluid has been streamlined as a new class of nanofluid, characterized by its thermal properties and potential utilities that serve the purpose of increasing the rate of heat transfer. Hybrid nanofluids are fluids that consist of two kinds of nanometer-sized particles, called nanoparticles dispersed in a base fluid. These hybrid nanofluids have numerous conceivable applications in all fields of heat transfer such as microfluidics, manufacturing, transportation, defence, medical, naval structures, acoustics and many more. Since then, many experimental and numerical research articles have been published with the concept of hybrid nanofluid. Momin [1] investigated experimentally the mixed convection flow in an inclined tube for hybrid nanofluid. They found that hybrid nanofluids show higher friction factor and Nusselt number when compared to pure water. Heat transfer enhancement of Ag-CuO/water hybrid nanofluid in the presence of heat generation, radiation and chemical reaction had been studied by Hayat and Nadeem [2]. Further, Manjunatha *et al.,* [3]

[*] *Corresponding author.*
E-mail address: nursyazana931@gmail.com (Nur Syazana Anuar)

analysed the effect of variable viscosity on heat transfer enhancement of hybrid nanofluid. Boundary layer flow and heat transfer over nonlinear stretching/shrinking surface in hybrid nanofluid was investigated by Waini *et al.,* [4]. Most of the researchers concluded that hybrid nanofluid flow plays a more substantial role in the process of heat transfer than a regular nanofluid flow. Also, the investigation of hybrid nanofluid has been reported by many researchers such as Tayebi and Chamkha [5], Ghadikolaei *et al.,* [6], Hamid *et al.,* [7], Ghalambaz *et al.,* [8], Waini *et al.,* [9] and Yıldız *et al.,* [10].

Much attention has been paid in the past decade to this new type of flow generated by a shrinking sheet due to its applications in industry such as hot rolling, metal extrusion and metal spinning, drawing of copper wires, glass fiber and many others. Miklavcic and Wang [11] were the first to investigate the viscous flow over a shrinking sheet. They observed that to maintain the flow of the shrinking sheet, mass suction is required. The stagnation point flow over the stretching/shrinking sheet in micropolar fluid with magnetohydrodynamic and slip effect has been investigated by Soid *et al.,* [12]. Later, Kamal *et al.,* [13] studied the effect of heat source on the stagnation point flow over stretching/shrinking sheet. While the MHD boundary layer flow over a stretching/shrinking wedge has been examined by Awaludin *et al.,* [14]. On the other hand, the flow of heat transfer over an exponentially shrinking sheet was first studied by Magyari and Keller [15]. Very recently, Anuar *et al.,* [16] investigated an exponentially vertical stretching/shrinking sheet of carbon nanotube with slip and suction effects. These authors have shown that there exists a dual solution for the case of a shrinking sheet. Afterward, the study of boundary layer flow over an exponentially stretching/shrinking sheet has been investigated by Rehman and Sheikh [17], Alavi *et al.,* [18], Jusoh *et al.,* [19], Anuar *et al.,* [20] and many more.

The present study is devoted to extending the work of Bachok *et al.,* [21] to the case permeable plate in a hybrid nanofluid. The implementation of suction and injection effects in this study can significantly change the flow field and eventually affect the heat transfer rate at the surface [22]. Using suitable similarity variables, ordinary differential equations are formulated and solved numerically using bvp4c package in Matlab software. The effect of governing parameters on fluid flow and heat transfer are illustrated graphically. The results obtained will then be examined to identify the stability of the solutions. We mention here the excellent papers on stability analysis by Merkin [23], Weidman *et al.,* [24], Harris *et al.,* [25], Najib *et al.,* [26], Anuar *et al.,* [27] and Naganthran *et al.,* [28].

2. Methodology

2.1 Mathematical Formulation

Let us consider the steady two-dimensional boundary layer flow of a hybrid nanofluid over an exponentially stretching/shrinking sheet with suction/injection effects. Figure 1 illustrates the flow configuration and coordinate system. Here, x is the coordinate measured along the sheet in a vertical direction and y is the coordinate measured in the direction normal to the sheet. The flow is assumed to be generated by stretching/shrinking sheet with velocity $U_w(x) = ae^{x/L}$ and inviscid flow velocity $U_\infty(x) = be^{x/L}$ where a, b are constants and L is a characteristic length of the sheet. It is also assumed that the temperature of the sheet is $T_w(x) = T_\infty + T_o e^{2x/L}$ where T_∞ is the temperature of the ambient fluid and T_o is the constant that measures the rate of temperature increase along the sheet. The velocity of the suction or injection is assumed to be $v_w(x) = -\left(\left(\nu_f b\right)/\left(2L\right)\right)^{1/2} e^{x/2L} s$ where

ν_f is the kinematic viscosity. It should also be mentioned that $s > 0$ is for suction and $s < 0$ is for injection. Hence, the governing equations of momentum and energy equations can be written as Bachok *et al.*, [21]

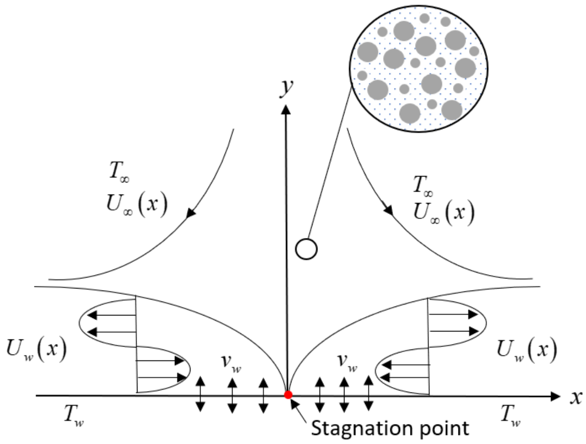

Fig. 1. Physical Model and Coordinate system

$$\frac{\partial u}{\partial x}+\frac{\partial v}{\partial y}=0 \tag{1}$$

$$u\frac{\partial u}{\partial x}+v\frac{\partial u}{\partial y}=U_\infty\frac{dU_\infty}{dx}+\frac{\mu_{hnf}}{\rho_{hnf}}\frac{\partial^2 u}{\partial y^2} \tag{2}$$

$$u\frac{\partial T}{\partial x}+v\frac{\partial T}{\partial y}=\alpha_{hnf}\frac{\partial^2 T}{\partial y^2} \tag{3}$$

and the associated boundary conditions are

$$\begin{aligned} &u=U_w(x),\;\; v=v_w(x),\;\; T=T_w(x) \quad \text{at } y=0\\ &u\to U_\infty(x),\;\; T\to T_\infty \qquad\qquad\quad \text{as } y\to\infty \end{aligned} \tag{4}$$

Here, μ_{hnf} is the dynamic viscosity of the hybrid nanofluid, ρ_{hnf} is the density of the hybrid nanofluid and α_{hnf} is the effective thermal diffusivity of hybrid nanofluid which are defined as [29]:

$$\begin{aligned} &\alpha_{hnf}=\frac{k_{hnf}}{\left(\rho C_p\right)_{hnf}},\mu_{hnf}=\frac{\mu_f}{(1-\varphi_1)^{2.5}(1-\varphi_2)^{2.5}},\; \rho_{hnf}=(1-\varphi_2)\left[(1-\varphi_1)\rho_f+\varphi_1\rho_{s1}\right]+\varphi_2\rho_{s2},\\ &\left(\rho C_p\right)_{hnf}=(1-\varphi_2)\left[(1-\varphi_1)\left(\rho C_p\right)_f+\varphi_1\left(\rho C_p\right)_{s1}\right]+\varphi_2\left(\rho C_p\right)_{s2},\\ &\frac{k_{hnf}}{k_{bf}}=\frac{k_{s2}+2k_{bf}-2\varphi_2\left(k_{bf}-k_{s2}\right)}{k_{s2}+2k_{bf}+\varphi_2\left(k_{bf}-k_{s2}\right)} \text{ where } \frac{k_{bf}}{k_f}=\frac{k_{s1}+2k_f-2\varphi_1\left(k_f-k_{s1}\right)}{k_{s1}+2k_f+\varphi_1\left(k_f-k_{s1}\right)} \end{aligned} \tag{5}$$

Where k is the thermal conductivity and ρC_p is the heat capacity where the subscript hnf, f, $s1$ and $s2$ represents hybrid nanofluid, fluid, CuO solid fraction and Ag solid fraction. Furthermore, φ_1

and φ_2 represent CuO and Ag nanoparticle volume fraction. It is worth to mention that hybrid nanofluids are formed by adding the mixture of Ag nanoparticles into a CuO/water nanofluid. The thermophysical properties of nanoparticles are illustrated in Table 1.

Table 1
Thermophysical properties of nanoparticle [2]

Physical Properties	Base fluid (Water)	CuO	Ag
$\rho\ (kg/m^3)$	997.1	6320	10500
$C_p\,(J/kgK)$	4 179	531.8	235
$k\,(W/mK)$	0.613	76.5	429
$\beta\times10^5\,(1/K)$	21	-	-

The dimensionless variables are introduced as:

$$\eta = y\left(\frac{b}{2\nu_f L}\right)^{1/2} e^{x/2L},\quad \psi = \left(2\nu_f Lb\right)^{1/2} f(\eta)e^{x/2L},\quad \theta(\eta) = \frac{T-T_\infty}{T_w-T_\infty} \tag{6}$$

where η is the similarity variable and the stream function ψ is defined as $u=\partial\psi/\partial y$ and $v=-\partial\psi/\partial x$, hence the equation of continuity, Eq. (1) is satisfied. By substituting Eq. (6) into governing equation from Eqs. (2)-(4), the non-dimensionless equations are obtained as follow:

$$\frac{\mu_{hnf}/\mu_f}{\rho_{hnf}/\rho_f} f''' + ff'' - 2f'^2 + 2 = 0 \tag{7}$$

$$\frac{1}{\Pr}\frac{k_{hnf}/k_f}{\left(\rho C_p\right)_{hnf}/\left(\rho C_p\right)_f}\theta'' + f\theta' - f'\theta = 0 \tag{8}$$

the corresponding boundary conditions are:

$$\begin{gathered} f(0)=s,\ \ f'(0)=\varepsilon,\ \ \theta(0)=1, \\ f'(\eta)\to 1,\ \ \theta(\eta)\to 0 \quad \text{as} \quad \eta\to\infty \end{gathered} \tag{9}$$

Here, prime denote differentiation with respect to η, Pr is the Prandtl number and $\varepsilon = a/b$ is the shrinking parameter with $\varepsilon < 0$.

The physical quantities of interest are skin friction coefficient and local Nusselt number which are defined as

$$C_f = \frac{\tau_w}{\rho_f U_\infty^2},\qquad Nu_x = \frac{2Lq_w}{k_f\left(T_w - T_\infty\right)} \tag{10}$$

where the surface shear stress τ_w and the heat flux q_w are given by

$$\tau_w = \mu_{hnf}\left(\frac{\partial u}{\partial y}\right)_{y=0}, \quad q_w = -k_{hnf}\left(\frac{\partial T}{\partial y}\right)_{y=0} \tag{11}$$

using the similarity variables (6), we obtain:

$$\mathrm{Re}_x^{1/2}\, C_f = \frac{\mu_{hnf}}{\mu_f} f''(0), \quad \mathrm{Re}_x^{-1/2}\, Nu_x = -\frac{k_{hnf}}{k_f}\theta'(0) \tag{12}$$

where $\mathrm{Re}_x = U_\infty x / \nu_f$ is the local Reynold number.

2.2 Flow Stability

We now investigate the stability of solutions by first considering the time-dependent problem (see Merkin [23]). Therefore, Eq. (1) holds, while Eqs. (2) and (3) are replaced by:

$$\frac{\partial u}{\partial t} + u\frac{\partial u}{\partial x} + v\frac{\partial u}{\partial y} = U_\infty \frac{dU_\infty}{dx} + \frac{\mu_{hnf}}{\rho_{hnf}}\frac{\partial^2 u}{\partial y^2} \tag{13}$$

$$\frac{\partial T}{\partial t} + u\frac{\partial T}{\partial x} + v\frac{\partial T}{\partial y} = \alpha_{hnf}\frac{\partial^2 T}{\partial y^2} \tag{14}$$

with the corresponding initial and boundary conditions:

$$\begin{aligned} &t<0 \quad u = v = 0, \ T = T_\infty \quad \text{for any } x, y \\ &t \ge 0 \quad u = U_w(x), \ v = v_w(x), \ T = T_w(x) \ \text{ at } \ y = 0 \\ &\qquad\ \ u \to U_\infty(x), \ T \to T_\infty \ \text{ as } \ y \to \infty \end{aligned} \tag{15}$$

where t denotes the time. The new variable τ and new non-dimensionless variables are introduced:

$$\eta = y\left(\frac{b}{2\nu_f L}\right)^{1/2} e^{x/2L}, \ \psi = \left(2\nu_f Lb\right)^{1/2} f(\eta,\tau) e^{x/2L}, \theta(\eta,\tau) = \frac{T-T_\infty}{T_w - T_\infty}, \quad \tau = \frac{bt}{2L}e^{x/2L} \tag{16}$$

using the similarity transformation in Eq. (16), the time-dependent governing equations in Eqs. (13) and (14) are transformed as follows:

$$\frac{\mu_{hnf}/\mu_f}{\rho_{hnf}/\rho_f}\frac{\partial^3 f}{\partial \eta^3} - 2\left(\frac{\partial f}{\partial \eta}\right)^2 + 2 + f\frac{\partial^2 f}{\partial \eta^2} - 2\tau\left(\frac{\partial f}{\partial \eta}\frac{\partial^2 f}{\partial \eta \partial \tau} - \frac{\partial f}{\partial \tau}\frac{\partial^2 f}{\partial \eta^2}\right) - \frac{\partial^2 f}{\partial \eta \partial \tau} = 0 \tag{17}$$

$$\frac{1}{\mathrm{Pr}}\frac{k_{hnf}/k_f}{(\rho C_p)_{hnf}/(\rho C_p)_f}\frac{\partial^2 \theta}{\partial \eta^2} + f\frac{\partial \theta}{\partial \eta} - \theta\frac{\partial f}{\partial \eta} - 2\tau\left(\frac{\partial f}{\partial \eta}\frac{\partial \theta}{\partial \tau} - \frac{\partial f}{\partial \tau}\frac{\partial \theta}{\partial \eta}\right) - \frac{\partial \theta}{\partial \tau} = 0 \tag{18}$$

subject to boundary conditions

$$f(0,\tau)=s,\quad \frac{\partial f}{\partial \eta}(0,\tau)=\varepsilon,\quad \theta(0,\tau)=1,$$
$$\frac{\partial f}{\partial \eta}(\eta,\tau)\to 1,\quad \theta(\eta,\tau)\to 0 \quad \text{as} \quad \eta\to\infty \tag{19}$$

The following term [24] are introduced:

$$f(\eta,\tau)=f_o(\eta)+e^{-\gamma\tau}F(\eta,\tau),\quad \theta(\eta,\tau)=\theta_o(\eta)+e^{-\gamma\tau}G(\eta,\tau) \tag{20}$$

Therefore, the stability solution $f(\eta)=f_o(\eta)$ and $\theta(\eta)=\theta_o(\eta)$ fulfilling the boundary-value problem can be identified where $F(\eta,\tau)$ and $G(\eta,\tau)$ are small relative to $f_o(\eta)$ and $\theta_o(\eta)$, while γ is an unknown eigenvalue.

Upon substituting Eq. (20) into Eqs. (17) and (18) along with the boundary conditions in Eq. (9), the new linearized problems are obtained. Setting $\tau=0$ as suggested by Weidman *et al.,* [24], eventually $F(\eta)=F_o(\eta)$ and $G(\eta)=G_o(\eta)$. Hence, we obtained the final equations as in the following form:

$$\frac{\mu_{hnf}/\mu_f}{\rho_{hnf}/\rho_f}F_o''' + f_oF_o'' + f_o''F_o-\left(4f_o'-\gamma\right)F_o'=0 \tag{21}$$

$$\frac{1}{\Pr}\frac{k_{hnf}/k_f}{\left(\rho C_p\right)_{hnf}/\left(\rho C_p\right)_f}G_o'' + f_oG_o'+F_o\theta_o'-F_o'\theta_o-G_of_o'+\gamma G_o=0, \tag{22}$$

the boundary conditions are now reduced to:

$$F_o(0)=0,\ F_o'(0)=0,\ \mathrm{G}_o(0)=0,$$
$$F_o'(\eta)\to 0,\ \mathrm{G}_o(\eta)\to 0,\ \text{as}\quad \eta\to\infty \tag{23}$$

The smallest eigenvalues γ can be determined by relaxing the boundary condition on $F_o(\eta)$ as suggested by Harris *et al.,* [25]. For the present research, the boundary conditions $F_o'(\eta)\to 0$ as $\eta\to\infty$ is relax and be replaced by new boundary condition $F_o''(0)=1$.

3. Results

The bvp4c solver in Matlab software is used to solve the system of ordinary differential equation from Eqs. (7) and (8) with the boundary conditions from Eq. (9). In order to validate the numerical results and the accuracy of the applied technique in the present problem, the comparison values of skin friction coefficient $f''(0)$ and heat transfer $-\theta'(0)$ for viscous fluid and $s=0$ are shown in Tables 2 and 3. It is clear that the obtained outcomes are in good agreement with the previously reported results of Bachok *et al.,* [21] and Subhashini *et al.,* [30]. The values of $f''(0)$ and $-\theta'(0)$

for hybrid nanofluid $(\varphi_1 = \varphi_2 = 0.1)$ are also included in these tables for future reference. Following Oztop and Abu-Nada [31], the values of nanoparticle volume fractions are varying from 0 to 0.2 $(0 < \varphi < 0.2)$ and Prandtl number is taken as 6.2 throughout the whole research. The effects of suction/injection parameter, nanoparticle volume fraction parameter and stretching/shrinking parameter on the dimensionless velocity, temperature, skin friction coefficient and local Nusselt number are demonstrated graphically and discussed in details. This research confirms the existence of non-unique solutions for a certain range of shrinking sheet $(\varepsilon \le -1)$ and unique solution when $-1 < \varepsilon \le 0$. However, there are no solution when $\varepsilon < \varepsilon_c$, where ε_c is a critical values of ε which depends on other parameters.

Table 2
Values of $f''(0)$ for some values of ε when $s = 0$ and $\Pr = 6.2$

φ_1	φ_2	ε	Bachok *et al.,* [21]	Subhashini *et al.,* [30]	Present results
0	0	-0.5	2.1182	2.1176	2.1182
		0	1.6872	1.6863	1.6872
0.1	0.1	-0.5	-	-	2.5391
		0	-	-	2.0225

Table 3
Values of $-\theta'(0)$ for some values of ε when $s = 0$ and $\Pr = 6.2$

φ_1	φ_2	ε	Bachok *et al.,* [21]	Present results
0	0	-0.5	0.6870	0.6870
		0	1.7148	1.7148
0.1	0.1	-0.5	-	0.8603
		0	-	1.4585

The effect of suction/injection parameter s on skin friction $f''(0)$ and velocity profile $f'(\eta)$ are shown in Figures 2 and 3. It is observed that in the case of hybrid nanofluid $(\varphi_1 = \varphi_2 = 0.1)$, the presence of suction $(s = 0.2)$ could increase the flow resistance, while injection $(s = -0.2)$ decreases the flow resistance for the first solution. Additionally, we observed contradictory behaviour for the second solution. Figures 4 and 5 present the performance of heat transfer $-\theta'(0)$ and temperature profile $\theta(\eta)$ for various values of suction/injection parameter s. Injection is discussed to inspect the rise in temperature, while suction depicts the reverse trends to cools the system for the first solution and vice versa for the second solution. It is further observed that when suction takes place in the boundary layer, the solution existence range is bound to increase and hence postponing the boundary layer separation. Also, it is seen that these profiles satisfied asymptotically the far field boundary conditions from Eq. (9).

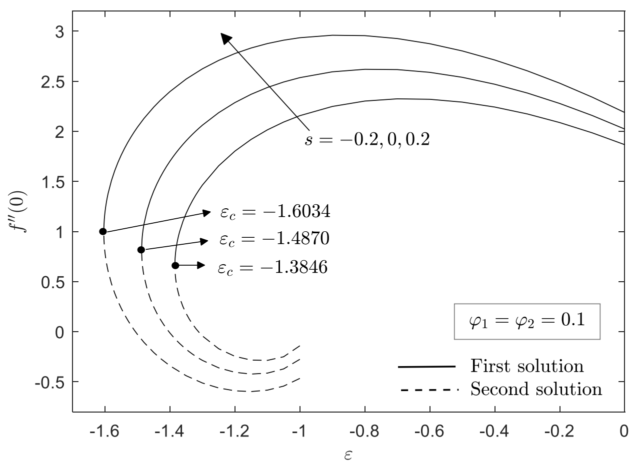

Fig. 2. Skin friction $f''(0)$ for different s

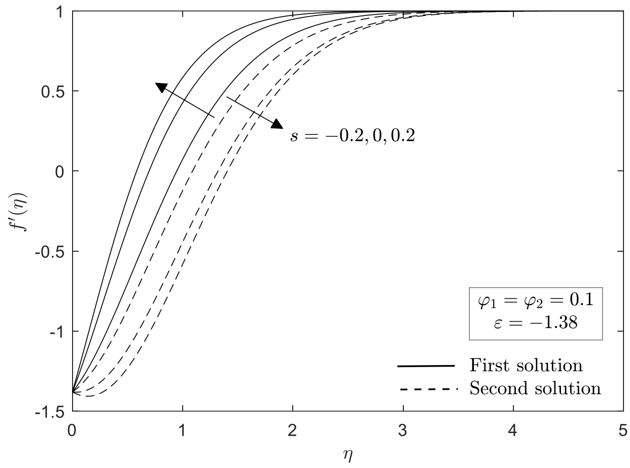

Fig. 3. Velocity profile $f'(\eta)$ for different s

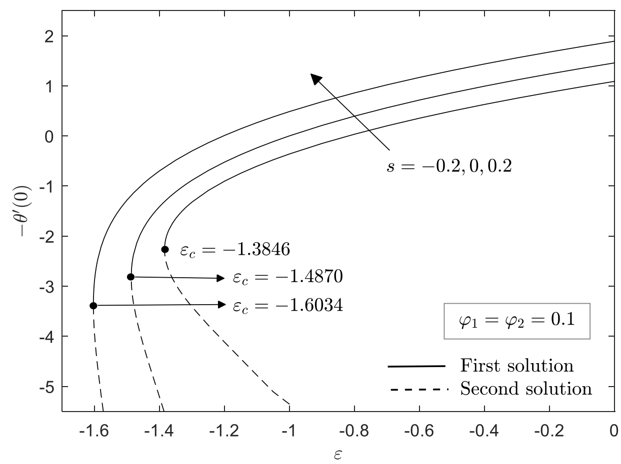

Fig. 4. Heat transfer $-\theta'(0)$ for different s

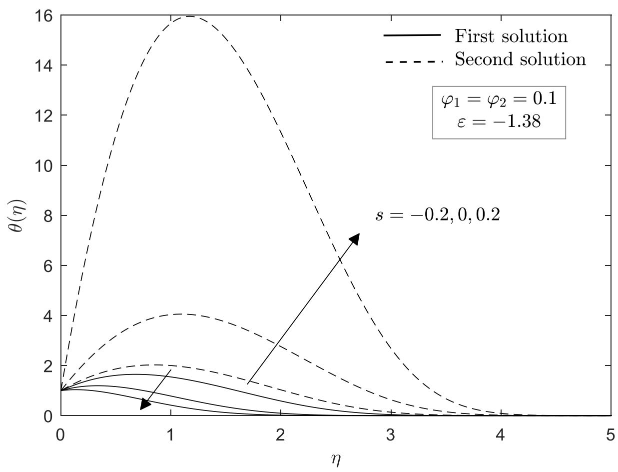

Fig. 5. Temperature profile $\theta(0)$ for different s

Figures 6 and 7 reflect the influence of Ag nanoparticle volume fraction φ_2 on skin friction and heat transfer in the presence of suction $(s=0.2)$. It is analysed that the skin friction and heat transfer increase by increasing values of Ag nanoparticle volume fraction. However, Figure 7 displayed the reverse trend when $\varepsilon > -0.8$. Moreover, it has been observed that the addition of nanoparticle volume fraction in nanofluid for suction case causes the postponing of boundary layer separation. The effect of Ag nanoparticle volume fraction in the presence of injection $(s=-0.2)$ on skin friction and heat transfer are shown in Figures 8 and 9. From these figures, it is found that the skin friction and heat transfer increase with the increasing values of Ag nanoparticle volume fraction. It is noticed that for the case of injection, the addition of Ag nanoparticle volume fraction in nanofluid tends to accelerate the boundary layer separation. It is important to note that hybrid nanofluid offers higher skin friction and heat transfer compared to nanofluid for both suction and injection case.

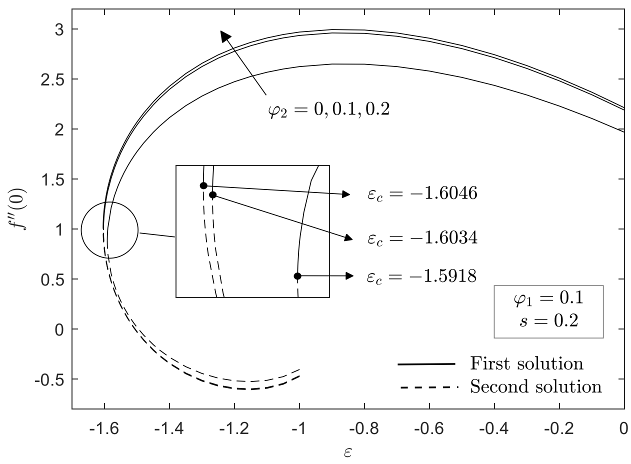

Fig. 6. Skin friction $f''(0)$ for different values of Ag nanoparticle volume fraction φ_2 when $s = 0.2$

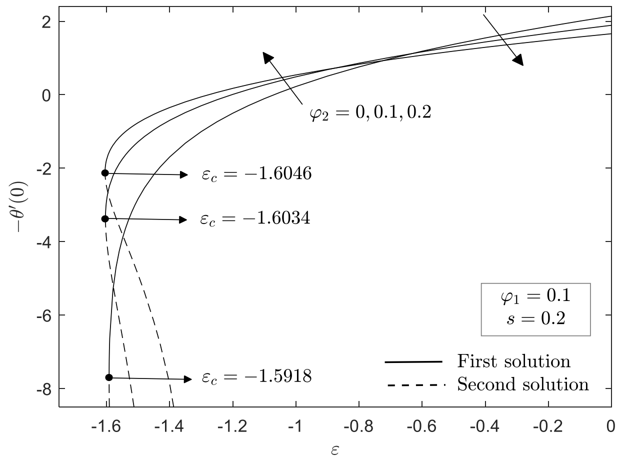

Fig. 7. Heat transfer $-\theta'(0)$ for different values of Ag nanoparticle volume fraction φ_2 when $s = 0.2$

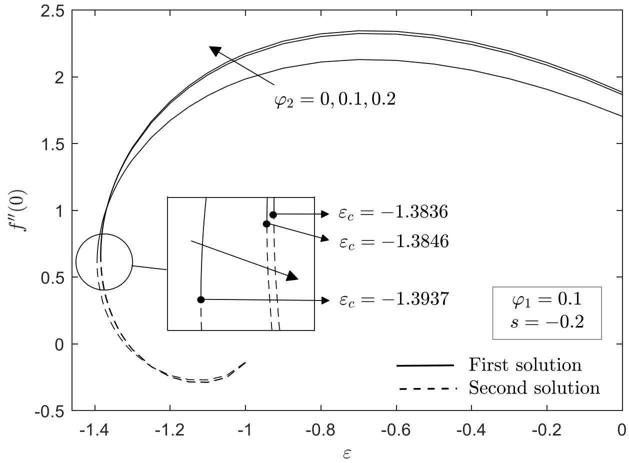

Fig. 8. Skin friction $f''(0)$ for different values of Ag nanoparticle volume fraction φ_2 when $s = -0.2$

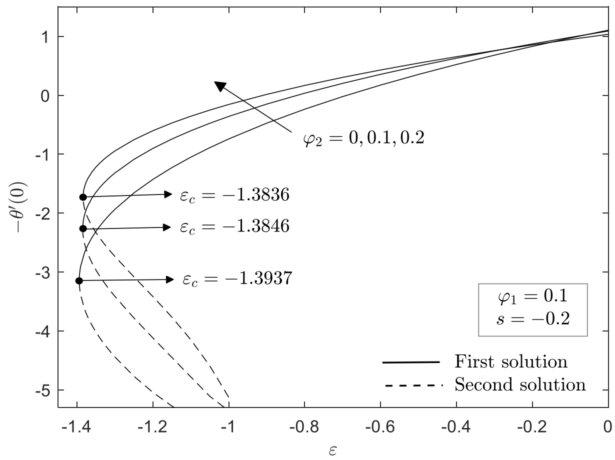

Fig. 9. Heat transfer $-\theta'(0)$ for different values of Ag nanoparticle volume fraction φ_2 when $s = -0.2$

The effects of suction/injection parameter s and nanoparticle volume fraction are depicted in Figures 10 and 11 for skin friction coefficient $\mathrm{Re}_x^{1/2} C_f$ and local Nusselt number $\mathrm{Re}_x^{-1/2} Nu_x$. It is witnessed that for increasing values of Ag nanoparticle volume fraction φ_2 and suction/injection parameter s, the skin friction coefficient and local Nusselt number increases. Also, the values of these quantities increase almost linearly with increasing values of CuO nanoparticle volume fraction φ_2. Figures 12 and 13 represent the effect of shrinking sheet on velocity $f'(\eta)$ and temperature profile $\theta(\eta)$ for the case of suction and hybrid nanofluid. It is found that with the increasing magnitude of the shrinking sheet, the velocity profile decreases for the first solution and increases for the second solution. Meanwhile, the temperature profile increase for the first solution and decreases for the second solution.

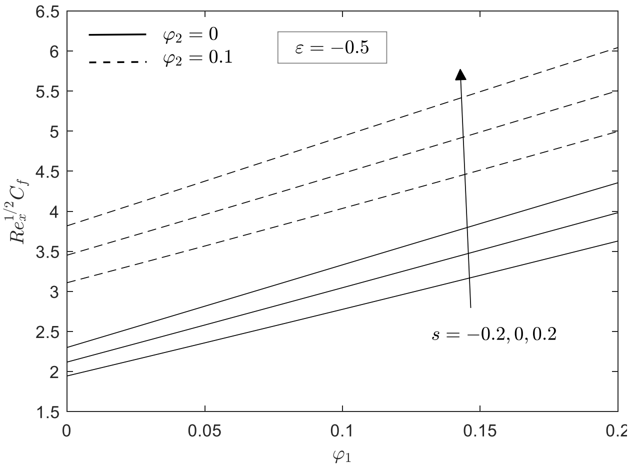

Fig. 10. Skin friction coefficient $\mathrm{Re}_x^{1/2} C_f$ for different values of s

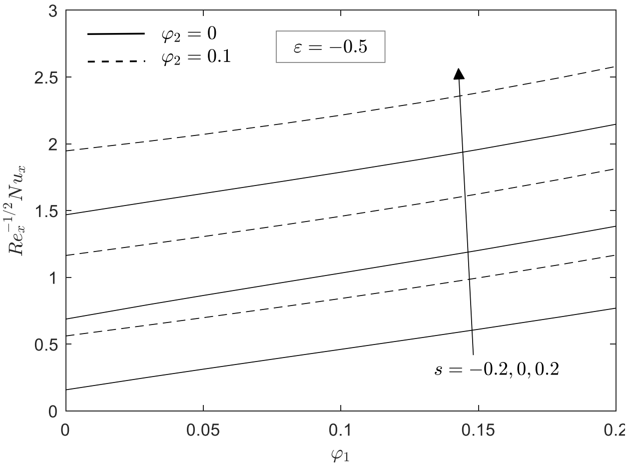

Fig. 11. Nusselt number $\mathrm{Re}_x^{-1/2} Nu_x$ for different values of s

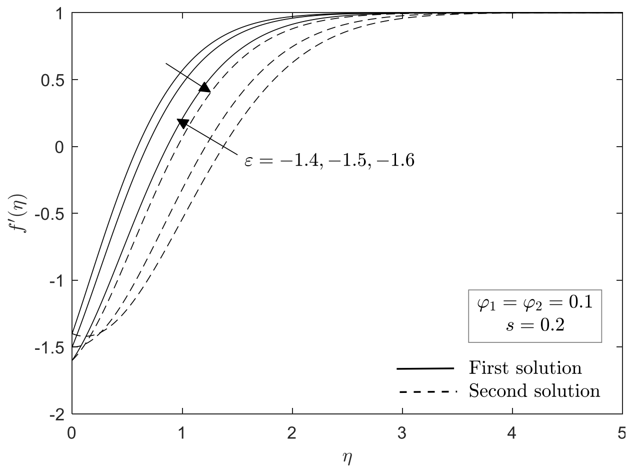

Fig. 12. Velocity profile $f'(\eta)$ for different values of shrinking parameter ε

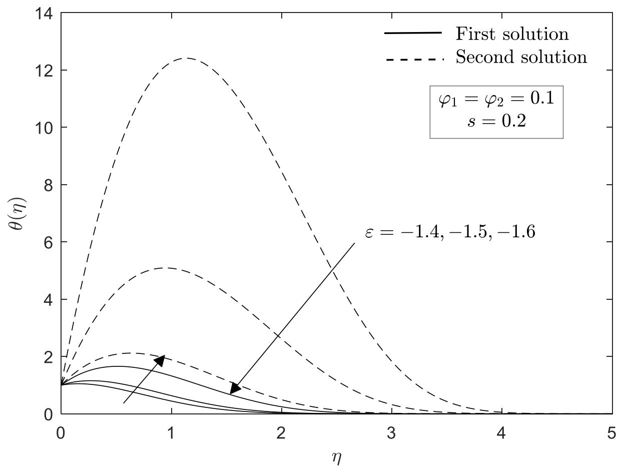

Fig. 13. Temperature profile $\theta(\eta)$ for different values of shrinking parameter ε

Since the obtained results are non-unique solutions, we are intended to do a stability analysis in order to identify which solution is stable and physically realizable. The system of linearized from Eqs. (21) and (22) along with the boundary condition in Eq. (23) are solved using the bvp4c solver in Matlab software to obtain the values of the smallest eigenvalues γ. Table 4 illustrates the smallest eigenvalues for the selected value of shrinking sheet, suction/injection parameter and Ag nanoparticle volume fraction when CuO nanoparticle volume fraction fixed to 0.1 volume fraction. These values are approaching zeros as the value of the shrinking parameter close to its critical value. Moreover, we can observe that the first solution presents positive values while the second solution shows the negative values. The positive value indicates that there exists only slight disturbance in the flow which does not interrupt the boundary layer separation and vice versa for the second solution. Hence, we can conclude that the first solution is stable meanwhile the second solution is unstable.

Table 4
Smallest eigenvalues γ for selected values of s, φ_2 and ε when $\varphi_1 = 0.1$

s	φ_2	ε	First solution	Second solution
-0.2	0	-1.3936	0.05739	-0.05733
		-1.393	0.13530	-0.13496
		-1.39	0.30584	-0.30414
	0.1	-1.3845	0.06184	-0.06177
		-1.384	0.12784	-0.12755
		-1.38	0.34170	-0.33958
0.2	0	-1.5917	0.06220	-0.06212
		-1.591	0.14597	-0.14556
		-1.59	0.21508	-0.21418
	0.1	-1.6033	0.05977	-0.05971
		-1.603	0.10509	-0.10488
		-1.6	0.29319	-0.29152

4. Conclusions

In the present study, the effect of suction/injection on the stagnation point flow over an exponentially shrinking sheet of hybrid nanofluid was studied numerically. From the numerical results obtained, some important conclusions are summarized:

i. The non-unique solutions exist for a certain range of the shrinking parameter $(\varepsilon \leq -1)$ and unique solutions when $\varepsilon > -1$.
ii. The suction parameter has a high impact on skin friction and heat transfer compared to injection parameter.
iii. The existence of suction parameter expands the range of solutions to exists and consequently delays the boundary layer separation.
iv. The increasing value of Ag nanoparticle volume fraction on CuO/water nanofluid causes increases in skin friction and heat transfer.
v. Hybrid nanofluid would give preferable heat transfer execution and skin friction when contrasted with nanofluid.
vi. For the case of suction, the range of solutions to exist increase with increasing value of Ag nanoparticle volume fraction and contradictory observations are made for the case of injection.
vii. Stability analysis ratifies the first solution as a stable solution and the second solution as an unstable solution.

Acknowledgement
This research was supported by a fundamental research grant scheme (FRGS/1/2018/STG06/UPM/02/4/5540155) and MyBrainsc from the Ministry of Higher Education Malaysia.

References
[1] Momin, and Gaffar G. "Experimental investigation of mixed convection with water-Al2O3 & hybrid nanofluid in inclined tube for laminar flow." *Int. J. Sci. Technol. Res* 2 (2013): 195-202.
[2] Hayat, Tanzila, and S. Nadeem. "Heat transfer enhancement with Ag–CuO/water hybrid nanofluid." *Results in physics* 7 (2017): 2317-2324.
[3] Manjunatha, S., B. Ammani Kuttan, S. Jayanthi, Ali Chamkha, and B. J. Gireesha. "Heat transfer enhancement in the boundary layer flow of hybrid nanofluids due to variable viscosity and natural convection." *Heliyon* 5, no. 4 (2019): e01469.

[4] Waini, Iskandar, Anuar Ishak, and Ioan Pop. "Hybrid nanofluid flow and heat transfer over a nonlinear permeable stretching/shrinking surface." *International Journal of Numerical Methods for Heat & Fluid Flow* 29, no. 9 (2019): 3110-3127.

[5] Tayebi, Tahar, and Ali J. Chamkha. "Buoyancy-driven heat transfer enhancement in a sinusoidally heated enclosure utilizing hybrid nanofluid." *Computational Thermal Sciences: An International Journal* 9, no. 5 (2017): 405-421.

[6] Ghadikolaei, S. S., M. Yassari, H. Sadeghi, Kh Hosseinzadeh, and D. D. Ganji. "Investigation on thermophysical properties of Tio2–Cu/H2O hybrid nanofluid transport dependent on shape factor in MHD stagnation point flow." *Powder technology* 322 (2017): 428-438.

[7] Hamid, K. Abdul, W. H. Azmi, M. F. Nabil, Rizalman Mamat, and K. V. Sharma. "Experimental investigation of thermal conductivity and dynamic viscosity on nanoparticle mixture ratios of TiO2-SiO2 nanofluids." *International Journal of Heat and Mass Transfer* 116 (2018): 1143-1152.

[8] Ghalambaz, Mohammad, Mikhail A. Sheremet, S. A. M. Mehryan, Farshad M. Kashkooli, and Ioan Pop. "Local thermal non-equilibrium analysis of conjugate free convection within a porous enclosure occupied with Ag–MgO hybrid nanofluid." *Journal of Thermal Analysis and Calorimetry* 135, no. 2 (2019): 1381-1398.

[9] Waini, Iskandar, Anuar Ishak, and Ioan Pop. "Unsteady flow and heat transfer past a stretching/shrinking sheet in a hybrid nanofluid." *International Journal of Heat and Mass Transfer* 136 (2019): 288-297.

[10] Yıldız, Çağatay, Müslüm Arıcı, and Hasan Karabay. "Comparison of a theoretical and experimental thermal conductivity model on the heat transfer performance of Al2O3-SiO2/water hybrid-nanofluid." *International Journal of Heat and Mass Transfer* 140 (2019): 598-605.

[11] Miklavčič, M., and Wang. C. "Viscous flow due to a shrinking sheet." *Quarterly of Applied Mathematics* 64, no. 2 (2006): 283-290.

[12] Soid, Siti Khuzaimah, Anuar Ishak, and Ioan Pop. "MHD stagnation-point flow over a stretching/shrinking sheet in a micropolar fluid with a slip boundary." *Sains Malaysiana* 47, no. 11 (2018): 2907-2916.

[13] Kamal, Fatinnabila, Khairy Zaimi, Anuar Ishak, and Ioan Pop. "Stability analysis on the stagnation-point flow and heat transfer over a permeable stretching/shrinking sheet with heat source effect." *International Journal of Numerical Methods for Heat & Fluid Flow* 28, no. 11 (2018): 2650-2663.

[14] Awaludin, Izyan Syazana, Anuar Ishak, and Ioan Pop. "On the stability of MHD boundary layer flow over a stretching/shrinking wedge." *Scientific reports* 8, no. 1 (2018): 13622.

[15] Magyari, E., and B. Keller. "Heat and mass transfer in the boundary layers on an exponentially stretching continuous surface." *Journal of Physics D: Applied Physics* 32, (1999): 577-585.

[16] Anuar, Nur Syazana, Norfifah Bachok, Norihan Md Arifin, and Haliza Rosali. "Mixed Convection Flow and Heat Transfer of Carbon Nanotubes Over an Exponentially Stretching/Shrinking Sheet with Suction and Slip Effect." *Journal of Advanced Research in Fluid Mechanics and Thermal Sciences* 59, no. 2 (2019): 232-242.

[17] Rehman, Abdul, and Naveed Sheikh. "Boundary Layer Stagnation-Point Flow of Micropolar Fluid over an Exponentially Stretching Sheet." *International Journal of Fluid Mechanics & Thermal Sciences* 3, no. 3 (2017): 25-31.

[18] Alavi, Sayed Qasim, Abid Hussanan, Abdul Rahman Mohd Kasim, Norhayati Rosli, and Mohd Zuki Salleh. "MHD Stagnation Point flow Towards an Exponentially Stretching Sheet with Prescribed wall Temperature and Heat Flux." *International Journal of Applied and Computational Mathematics* 3, no. 4 (2017): 3511-3523.

[19] Jusoh, Rahimah, Roslinda Nazar, and Ioan Pop. "Magnetohydrodynamic rotating flow and heat transfer of ferrofluid due to an exponentially permeable stretching/shrinking sheet." *Journal of Magnetism and Magnetic Materials* 465 (2018): 365-374.

[20] Anuar, Nur Syazana, Norfifah Bachok, Norihan Md Arifin, and Haliza Rosali. "Stagnation Point Flow and Heat Transfer over an Exponentially Stretching/Shrinking Sheet in CNT with Homogeneous–Heterogeneous Reaction: Stability Analysis." *Symmetry* 11, no. 4 (2019): 522.

[21] Bachok, Norfifah, Anuar Ishak, and Ioan Pop. "Boundary layer stagnation-point flow and heat transfer over an exponentially stretching/shrinking sheet in a nanofluid." *International Journal of Heat and Mass Transfer* 55, no. 25-26 (2012): 8122-8128.

[22] Al-Sanea, Sami A. "Mixed convection heat transfer along a continuously moving heated vertical plate with suction or injection." *International Journal of Heat and Mass Transfer* 47, no. 6-7 (2004): 1445-1465.

[23] Merkin, J. H. "On dual solutions occurring in mixed convection in a porous medium." *Journal of engineering Mathematics* 20, no. 2 (1986): 171-179.

[24] Weidman, P. D., D. G. Kubitschek, and A. M. J. Davis. "The effect of transpiration on self-similar boundary layer flow over moving surfaces." *International journal of engineering science* 44, no. 11-12 (2006): 730-737.

[25] Harris, S. D., D. B. Ingham, and I. Pop. "Mixed convection boundary-layer flow near the stagnation point on a vertical surface in a porous medium: Brinkman model with slip." *Transport in Porous Media* 77, no. 2 (2009): 267-285.

[26] Najib, Najwa, Norfifah Bachok, Norihan Md Arifin, and Fadzilah Md Ali. "Stability analysis of stagnation point flow in nanofluid over stretching/shrinking sheet with slip effect using buongiorno's model." *Numerical Algebra, Control & Optimization* 9, no. 4 (2019): 423-431.

[27] Anuar, Nur, Norfifah Bachok, and Ioan Pop. "A stability analysis of solutions in boundary layer flow and heat transfer of carbon nanotubes over a moving plate with slip effect." *Energies* 11, no. 12 (2018): 3243.

[28] Naganthran, Kohilavani, Roslinda Nazar, and Ioan Pop. "Effects of thermal radiation on mixed convection flow over a permeable vertical shrinking flat plate in an Oldroyd-B fluid." *Sains Malaysiana* 47, no. 5 (2018): 1069-1076.

[29] Devi, S. Suriya Uma, and SP Anjali Devi. "Numerical investigation of three-dimensional hybrid Cu–Al2O3/water nanofluid flow over a stretching sheet with effecting Lorentz force subject to Newtonian heating." *Canadian Journal of Physics* 94, no. 5 (2016): 490-496.

[30] Subhashini, S. V., R. Sumathi, and E. Momoniat. "Dual solutions of a mixed convection flow near the stagnation point region over an exponentially stretching/shrinking sheet in nanofluids." *Meccanica* 49, no. 10 (2014): 2467-2478.

[31] Oztop, Hakan F., and Eiyad Abu-Nada. "Numerical study of natural convection in partially heated rectangular enclosures filled with nanofluids." *International journal of heat and fluid flow* 29, no. 5 (2008): 1326-1336.